CHANNELS
2017, VOL. 11, NO. 6, 555–573
https://doi.org/10.1080/19336950.2017.1356954

Taylor & Francis
Taylor & Francis Group

RESEARCH PAPER

Ca_V2 channel subtype expression in rat sympathetic neurons is selectively regulated by $\alpha_2\delta$ subunits

Mallory B. Scott[a] and Paul J. Kammermeier[b]

[a]Departments of Biochemistry and Biophysics, University of Rochester Medical Center, Rochester, NY, USA; [b]Departments of Pharmacology and Physiology, University of Rochester Medical Center, Rochester, NY, USA

ABSTRACT

Type two voltage gated calcium (Ca_V2) channels are the primary mediators of neurotransmission at neuronal presynapses, but their function at neural soma is also important in regulating excitability.[1] Mechanisms that regulate Ca_V2 channel expression at synapses have been studied extensively, which motivated us to perform similar studies in the soma. Rat sympathetic neurons from the superior cervical ganglion (SCG) natively express $Ca_V2.2$ and $Ca_V2.3$.[2] We noted previously that heterologous expression of $Ca_V2.1$ but not $Ca_V2.2$ results in increased calcium current in SCG neurons.[3] In the present study, we extended these observations to show that both $Ca_V2.1$ and $Ca_V2.3$ expression resulted in increased calcium currents while $Ca_V2.2$ expression did not. Further, $Ca_V2.1$ could displace native $Ca_V2.2$ channels, but $Ca_V2.3$ expression could not. Heterologous expression of the individual accessory subunits $\alpha_2\delta$-1, $\alpha_2\delta$-2, $\alpha_2\delta$-3, or β4 alone failed to increase current density, suggesting that the calcium current ceiling when $Ca_V2.2$ was over-expressed was not due to lack of these subunits. Interestingly, introduction of recombinant $\alpha 2\delta$ subunits produced surprising effects on displacement of native $Ca_V2.2$ by recombinant channels. Both $\alpha_2\delta$-1 and $\alpha_2\delta$-2 seemed to promote $Ca_V2.2$ displacement by recombinant channel expression, while $\alpha_2\delta$-3 appeared to protect $Ca_V2.2$ from displacement. Thus, we observe a selective prioritization of Ca_V channel functional expression in neurons by specific $\alpha_2\delta$ subunits. These data highlight a new function for $\alpha_2\delta$ subtypes that could shed light on subtype selectivity of Ca_V2 membrane expression.

ARTICLE HISTORY
Received 3 May 2017
Revised 13 July 2017
Accepted 13 July 2017

KEYWORDS
calcium channels; patch-clamp; sympathetic neurons

Introduction

Type two voltage gated calcium channels (Ca_V2) are found throughout the central and peripheral nervous systems. The most well-described function of these channels is to mediate presynaptic calcium entry and initiate neurotransmission, but in neurons Ca_V2 channels express in the somatodendritic compartment as well, where they can regulate excitability either directly or via coupling to calcium dependent potassium and chloride channels.[1,4] There are three Ca_V2 subtypes, each defined by the sequence of the $Ca_V\alpha1$ pore-forming subunit: $Ca_V2.1$ ($Ca_V\alpha1A$), $Ca_V2.2$ ($Ca_V\alpha1B$) and $Ca_V2.3$ ($Ca_V\alpha1E$). The channel is comprised of four domains that form a calcium selective pore, voltage sensing domains, and regions that open and close the channels. $Ca_V2.1$ and $Ca_V2.2$ play dominant roles in neurotransmission in the nervous system, as they directly associate with presynaptic proteins SNAP-25 and syntaxin.[5,6] Ca_V2 channels can also couple to the calmodulin kinase (CaMK) nuclear signaling cascade that occurs in the somatodendritic region of the cell, resulting in increased phosphorylation of cAMP response binding protein (CREB), although with lower sensitivity than Ca_V1 channels.[7,8]

The dependency on cellular localization for the function of these channels has prompted extensive research to understand how and where the channel subtypes are trafficked in the various neuronal compartments. To be trafficked to the membrane, the $Ca_V\alpha1$ subunit associates with auxiliary subunits β and $\alpha_2\delta$.[9] There are multiple subtypes of these auxiliary subunits, including β1-4 and $\alpha_2\delta$-1-4.[4] With the exception of $\alpha_2\delta$-4, which is predominately retinal and auditory, all subtypes of auxiliary subunits are found within the central and peripheral nervous system at varying expression levels.[10,11] Functionally, the β subunit associates with the $\alpha1$ subunit at the endoplasmic reticulum to ensure proper folding of the channel

CONTACT Paul J. Kammermeier paul_kammermeier@urmc.rochester.edu Department of Pharmacology and Physiology, University of Rochester Medical Center, Box 711, 601 Elmwood Ave., Rochester, NY 14642, USA.

complex, allowing the complex to be trafficked through the secretory pathway.[12,13] The role of $\alpha_2\delta$ is more complex. Co-expression of $\alpha_2\delta$ potentiates surface expression of $\alpha1/\beta$ channel complex in most systems.[14] Additionally, $\alpha_2\delta$ and β with $\alpha1$ may also alter channel biophysical properties such as inactivation and channel gating.[9] In general, any combination of $\alpha_2\delta$, β and $\alpha1$ subunit will result in enhanced trafficking of the complex to the membrane.[9]

Incoming calcium is highly buffered in a cell.[15] Thus, regulating the amount of channels that are trafficked to the plasma membrane is essential to assure proper function.[16] In exploring how neurotransmission is affected by recombinant channel expression, Mochida et al. demonstrated that recombinant Ca_V2 subtypes reconstituted synaptic transmission similarly to native Ca_V2 channels in rat superior cervical ganglion.[17] What remained to be identified was how the recombinant channels were limited at the presynapse, as overexpression of the channels did not enhance the synaptic transmission. In 2004, Cao and Tsien hypothesized that "slots," or expression limits due to some unidentified mechanisms, regulated the relative amount of recombinant channels at the presynapse in a subtype dependent manner.[18] Interestingly, $Ca_V2.2$ mediated current was not reduced by overexpression of recombinant $Ca_V2.1$.[19] Others have described a direct mechanism to explain these observations. For example, Hoppa et al. argue that limitations in auxiliary Ca_V2 subunits create a bottleneck for channels to be trafficked from the soma to presynapse. However, clearly specific effects of different $\alpha2\delta$ subunits were not observed, and effects of distinct $\alpha2\delta$ subunits on specific expressed Ca_V channels were not tested.[20]

In this study, the goal was to examine Ca_V2 channel expression on the somatic membrane of rat superior cervical ganglion (SCG) neurons. By examining somatic rather than presynaptic channels, we hoped to reduce the variables as presynaptic trafficking requires more protein interactions. Further, we seek to determine if there is a general mechanism for subtype selectivity for functional channel expression. We found that recombinant channel expression in SCG neurons from adult rats have expression level limits that are Ca_V2 subtype specific. The general observations were that recombinant $Ca_V2.2$ has a "ceiling," or an upper limit of membrane expression similar to the native expression levels. Conversely, overexpression of $Ca_V2.1$ and $Ca_V2.3$ resulted in an increase in the number of channels trafficked to the plasma membrane, thus did not appear to be restricted in the same way as $Ca_V2.2$. Recombinant $Ca_V2.1$, but not $Ca_V2.3$ expression, reduced the amount of native $Ca_V2.2$ channels on the plasma membrane. Interestingly, we found that displacement appeared to depend on $\alpha_2\delta$ subunits in a selective way. Expression of $\alpha_2\delta$-1 permitted $Ca_V2.3$ to displace native $Ca_V2.2$ channels while $\alpha_2\delta$-3 protected $Ca_V2.2$ from displacement by other channels, and only $\alpha_2\delta$-2 was associated with a significant increase in current when $Ca_V2.2$ was overexpressed, either due to relief of the observed ceiling, or by allowing these channels to be expressed via another pathway. These findings show a novel function of $\alpha_2\delta$ subtypes, conferring selectivity on recombinant Ca_V2 channel subtypes for preferential expression on the plasma membrane.

Results

Recombinant $Ca_V2.1$ and $Ca_V2.3$, but not $Ca_V2.2$ increase total ICa

Previously, we showed that heterologous expression of $Ca_V2.1$ in SCG neurons results in an increase in total calcium current density,[3] in agreement with previous reports examining hippocampal neurons.[18] Adult rat SCG neurons natively express $Ca_V2.2$ and $Ca_V2.3$, with $Ca_V2.2$ mediating approximately 60–75% of the calcium current.[2] Heterologous expression of $Ca_V2.1$ in SCG neurons produced an increase in current without co-expression of $\alpha_2\delta$ and β subunits. This was likely due to the fact that SCG neurons are adult, differentiated neurons that natively express these accessory subunits, which can apparently support recombinant expression of $Ca_V2.1$. Interestingly however, recombinant $Ca_V2.2$ expression did not result in enhanced current.[3] In the present study, we examined in more detail the selectivity of functional expression of Ca_V2 channels in SCG neurons. Overexpression was achieved by intra-nuclear injection of cDNA encoding the α_1 pore-forming subunit of each Ca_V2 channel (with EGFP) into primary cultures of SCG neurons.[21] Using whole-cell patch-clamp electrophysiology, the relative amount of functional channels on the plasma membrane in each expression condition was determined by application of 80 msec voltage steps ranging from −80 mV to +60 mV in 10 mV increments from a holding potential of −80 mV. The calcium currents were measured 10 msec after the

start of each step, at or near steady-state levels, normalized to cell capacitance and plotted against voltage to generate a current voltage (IV) curve.[22] Currents did not appreciably inactivate during this time. Fig. 1A shows raw calcium current trace (I_{ca}) elicited from −70, −10 and +10 mV steps from cells in each overexpression condition. When $Ca_V2.2$ (rabbit α_{1B}) was overexpressed the current response did not change significantly compared to uninjected cells (Fig. 1B) suggesting that there is some limit or ceiling for $Ca_V2.2$ membrane expression. HEK293 cells transfected with the same $Ca_V2.2$ plasmid (with $\beta4$ and $\alpha_2\delta$-1) resulted in measurable calcium current, demonstrating that a functional channel is properly translated and trafficked to the plasma membrane (Fig. 1E). Expression of recombinant non-conductive $Ca_V2.2$ ("$NCCa_V2.2$") reduced the current density below uninjected levels, suggesting that recombinant $Ca_V2.2$ protein can express in SCG neurons where it appears to displace at least some native channels either at the level of the plasma membrane or during trafficking (Fig. 1C). Because splice isoforms of exon 37 of $Ca_V2.2$ can affect expression levels,[23] we examined calcium current densities in cells expressing mouse $Ca_V2.2$ with the two mutually exclusive exons, 37a and b (mouse α_{1B}). As expected, mouse $Ca_V2.2\_37a$ increased current density while $Ca_V2.2\_37b$ did not, consistent with our results using the rabbit clone (Fig. 1D). It should be noted that the 37b splice isoform is the dominant variant expressed in SCG neurons,[23] and the increased current observed with 37a is probably due to enhanced association with the adaptor protein AP-1, likely a separate mechanism than that regulating the $Ca_V2.2$ ceiling in SCG neurons[24] because the 37a isoform is relevant to nociceptive neurons but is not expressed in sympathetic neurons.

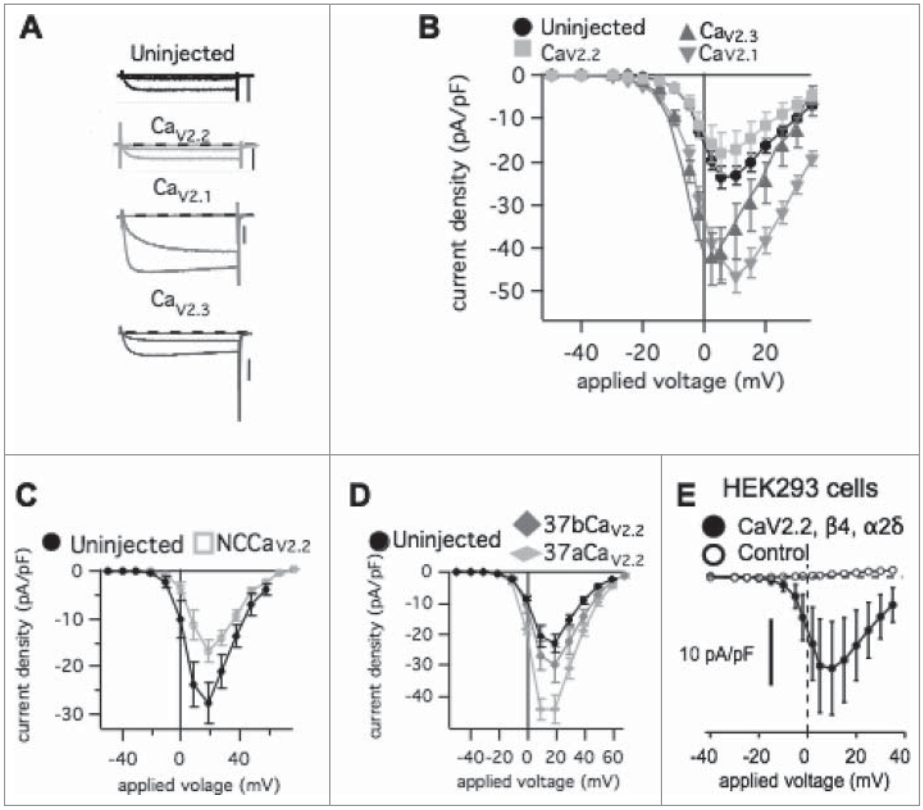

Figure 1. Effect of heterologous expression of Ca_{V2} channel $\alpha1$ subunits on total calcium current density in rat SCG neurons. (A), Sample calcium current current traces during 80 msec steps to −70 mV, −10 mV, and +10 mV from a holding potential of -80 mV in SCG neurons with the indicated expression. Scale bars in each represent 2 nA. (B), Current-voltage (IV) relations for SCG neurons (average ± SEM) either uninjected (•; n = 20), or expressing $Ca_V2.1$ (▼; n = 14), $Ca_V2.2$ (□; n = 18), or $Ca_V2.3$ (▲; n = 14). (C), Current-voltage (IV) relations (average ± SEM) for uninjected (•; n = 5) SCG neurons and cells expressing $NCCa_V2.2$ (□; n = 10). (D), Current-voltage (IV) relations (average ± SEM) for uninjected (•; n = 8) SCG neurons and cells expressing exon 37 splice variants of $Ca_V2.2$, 37a (◆□; n = 9) or 37b (◆□; n = 9). (E), Current-voltage relationship (I-V curves) for control HEK293 cells (untransfected) (○), and those transfected with $\beta4$, $\alpha2\delta$-1, and the same $Ca_V2.2$ construct used in the experiments described in Figure 1B (n = 3; ●).

Thus the $Ca_V2.2$ ceiling observed in our system is pertinent feature unique to SCG neurons $Ca_V2.2$ with exon 37b, and is consistent with two separate $Ca_V2.2$ constructs. Finally, expression of GFP alone did not alter the current compared to uninjected cells (not shown).

In contrast to the $Ca_V2.2$ results, $Ca_V2.1$ (rat α_{1A}) and $Ca_V2.3$ (mouse α_{1E}) overexpression resulted in significantly enhanced current densities, suggesting that more channels were localized to the plasma membrane when these subtypes were recombinantly expressed (Fig. 1B). In the context of current density values from a large number (>1000) of SCG neurons under similar recording conditions, it seems implausible that the increase in current density occurs by chance or by selection bias (Fig. 2). Together these data suggest that $Ca_V2.1$ and $Ca_V2.3$ are not limited by the same expression ceiling as $Ca_V2.2$ in SCG neurons, and that there likely are separate mechanisms limiting these subtypes in their trafficking and stability at the plasma membrane.

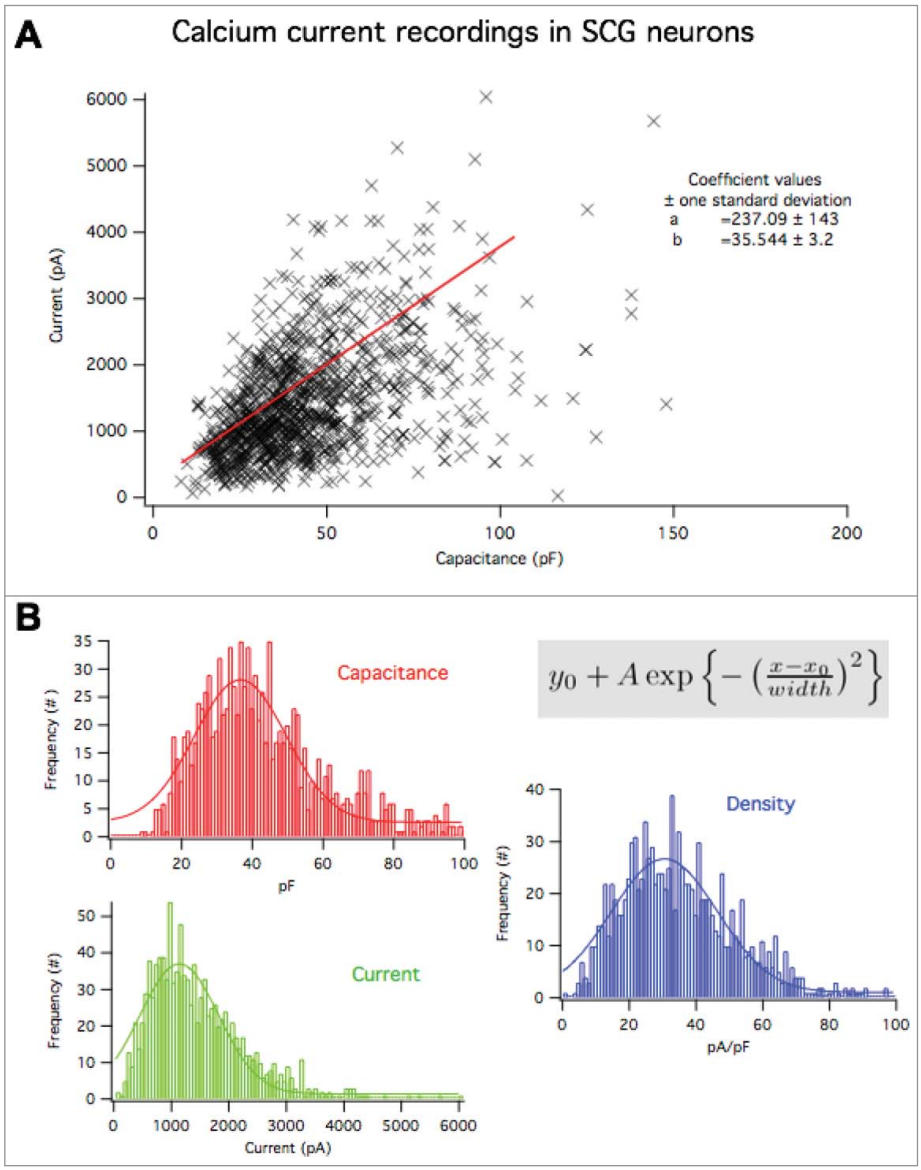

Figure 2. Distribution of whole cell capacitance, whole cell calcium currents, and current density in 1108 SCG neurons under the recording conditions employed in this study. (A), relationship between whole cell calcium current and cell capacitance. Plot shows the value from each cell (X), and a linear regression to all of the data yielding a slope of 36 ± 3 pA/pF. (B), Histograms showing the frequency distributions of whole cell capactiance (red), whole cell calcium current (green) and current density (blue) of the cells in (A). These data were fit to a Gaussian distribution of the form illustrated in the *inset*. Fits are shown as solid lines and yielded the following values: For capacitance: $Y_o = 0.50 \pm 0.19$; $A = 6.0 \pm 0.5$; $X_o = 36.3 \pm 1.4$; *width* $= 21 \pm 2.4$. For current: $Y_o = 0.17 \pm 0.2$; $A = 5.9 \pm 0.5$; $X_o = 0.05 \pm 0.04$; *width* $= 0.23 \pm 0.05$. For current density: $Y_o = 0.21 \pm 0.15$; $A = 8.5 \pm 0.4$; $X_o = -2.8 \pm 0.14$ *width* $= 2.7 \pm 0.2$.

Recombinant $Ca_V2.1$ displaces native $Ca_V2.2$, but recombinant $Ca_V2.3$ does not

We next investigated if there was competition between recombinant and native channels similar to that reported for some Ca_V2 channels expressed at presynaptic sites.[19] To determine the amount of each Ca_V2 subtype contributing to the total calcium current, one or more selective pharmacological inhibitors were perfused on the cell while a voltage ramp (−120 mV to 80 mV in 160 msec, V_{hold} = −80 mV) was applied every ten seconds. These data are depicted using dot plots in which open symbols denote the current density before drug application, and closed symbols denote the current in the presence of the blocker. Lines connect peak current densities from individual cells before and after drug application. Average ± SEM values are shown as horizontal lines with vertical error bars. In cells expressing $Ca_V2.3$ we observed a large decrease (reduced by 29 ± 7 pA/pF; n = 5) of calcium current in the presence of the $Ca_V2.3$ specific blocker SNX-482 (1 μM),[25] while uninjected cells exhibited a much smaller decrease of current density (reduced by 5.4 ± 1 pA/pF n = 6) by SNX-482 (Fig. 3A). Overexpression of a non-conductive $Ca_V2.3$ ("$NCCa_V2.3$"), in which all four calcium coordinating

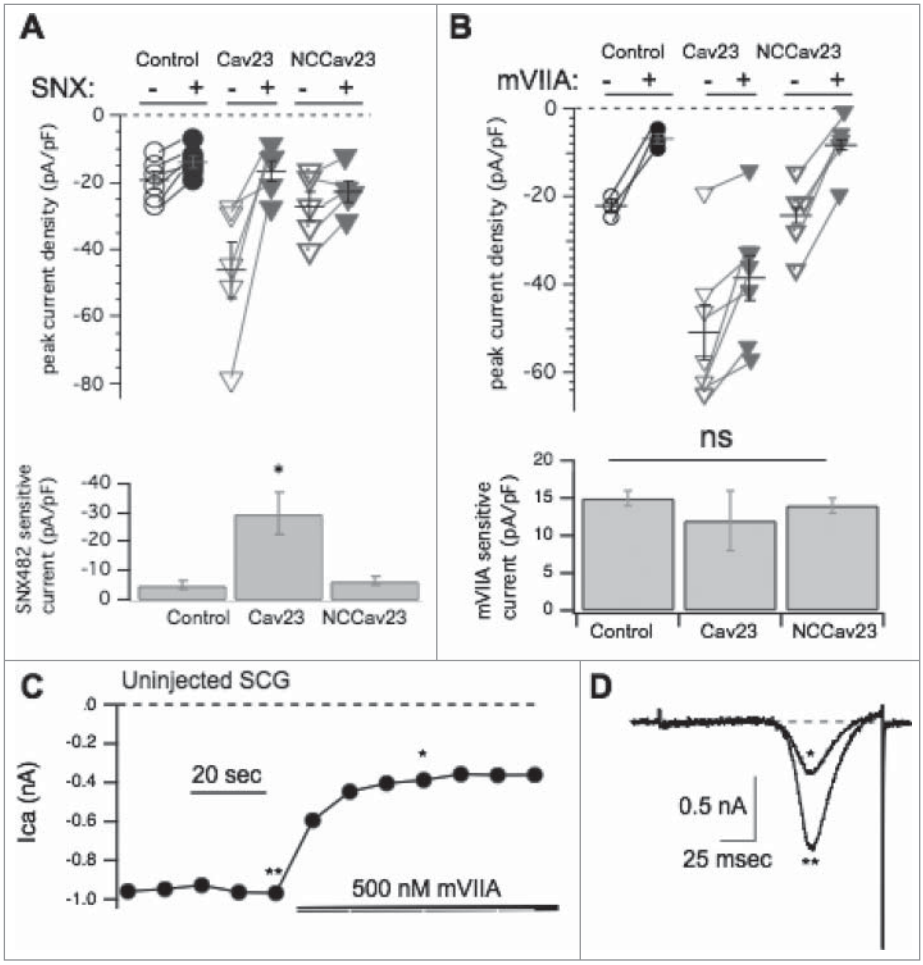

Figure 3. Pharmacological dissection of enhanced calcium currents when $Ca_{V2.3}$ is expressed in SCG neurons. (A), *Upper*, Summary of control (open, -) and SNX482 inhibited (filled, +) current amplitudes in uninjected (○, •; n = 6), $Ca_V2.3$- (n = 5), and $NCCa_{V2.3}$-expressing (▽, ▼; n = 5) SCG neurons. Averages ± standard errors are also indicated as black lines with error bars for each group. *Lower*, Bar graph illustrating average (±SEM) current density inhibited by SNX482 (total – remaining current) in each group. * indicates $p < 0.05$. (B), *Upper*, Summary of control (open, -) and ω-conotoxin mVIIA- inhibited (filled, +) current amplitudes in uninjected (○, •; n = 3), $Ca_V2.3$- (n = 7), and $NCCa_V2.3$-expressing (▽, ▼; n = 5) SCG neurons. Averages ± standard errors are also indicated as black lines with error bars for each group. *Lower*, Bar graph illustrating average (±SEM) current density inhibited by ω-conotoxin mVIIA (total – remaining current) in each group. ns indicates that no significant differences were detected. (C), Sample current amplitude time course for an uninjected, control SCG neuron during application of ω-conotoxin mVIIA. Points represent peak inward currents from a ramp voltage protocol from -120 to +80 mV, as in (D). (D), Sample current traces illustrating uninhibited current (**) and ω-conotoxin mVIIA inhibited current (*) from the same cell depicted in (C).

glutamate residues in in the channel pore were mutated to alanine, did not result in a significant enhancement or reduction of the SNX-482 sensitive current (Fig. 3A) compared to uninjected cells, with a reduction of 6.4 ± 1 pA/pF (n = 5) upon SNX-482 application (Fig. 3B). Overall, expression of $Ca_V2.3$ increased the calcium current density, but the result of the $NCCa_V2.3$ experiment suggested that recombinant $Ca_V2.3$ channels did not appear to displace native $Ca_V2.3$, suggesting that under native conditions these channels are not expressed at or very near a ceiling as $Ca_V2.2$ appears to be.

Moreover, recombinant $Ca_V2.3$ did not reduce the amount of $Ca_V2.2$ current. As shown in Fig. 3B, no significant change was observed in the amount of current sensitive to 500 nM ω-conotoxin mVIIA, a $Ca_V2.2$ specific blocker, when $Ca_V2.3$ was expressed.[26] ω-conotoxin mVIIA reduced the current in uninjected cells by 14 ± 1 pA/pF (n = 9). A time course of block in an uninjected SCG neuron is shown in Fig. 3C, with sample ramp current traces from that cell shown in Fig. 3D. The currents illustrated are indicated by asterisks (** = the control, unblocked current, * = current inhibited by ω-conotoxin mVIIA). Application of ω-conotoxin mVIIA reduced the current by 12 ± 3 pA/pF (n = 7) in cells expressing $Ca_V2.3$ (Fig. 3B). When $NCCa_V2.3$ was overexpressed a reduction of 14 ± 1 pA/pF (n = 9) by ω-conotoxin mVIIA was observed (Fig. 3B), a value indistinguishable from control and $Ca_V2.3$ expressing cells. Thus, the amount of $Ca_V2.2$-specific current is not significantly different between functional $Ca_V2.3$, $NCCa_V2.3$ or uninjected conditions. These data indicate that recombinant $Ca_V2.3$ does not compete with native channels for membrane expression.

To examine the effects of $Ca_V2.1$ on subtype specific expression, similar experiments were conducted in $Ca_V2.1$ expressing SCG neurons using the $Ca_V2.1$ selective blocker ω-agatoxin IVA[27] (500 nM) and ω-conotoxin mVIIA (500 nM). As expected, recombinant $Ca_V2.1$ overexpression resulted in significantly more $Ca_V2.1$ (ω-agatoxin IVA sensitive) calcium current, 46 ± 8 pA/pF (n = 6) in $Ca_V2.1$ expressing cells, from nearly undetectable, 2.1 ± 0.3 pA/pF (n = 6) in uninjected cells (Fig. 4B; p = 0.0003 by Student's t-test). Note that in this figure, the open and closed symbol convention used in the other figures was replaced with all open symbols of varying sizes to better illustrate the many overlapping points, especially

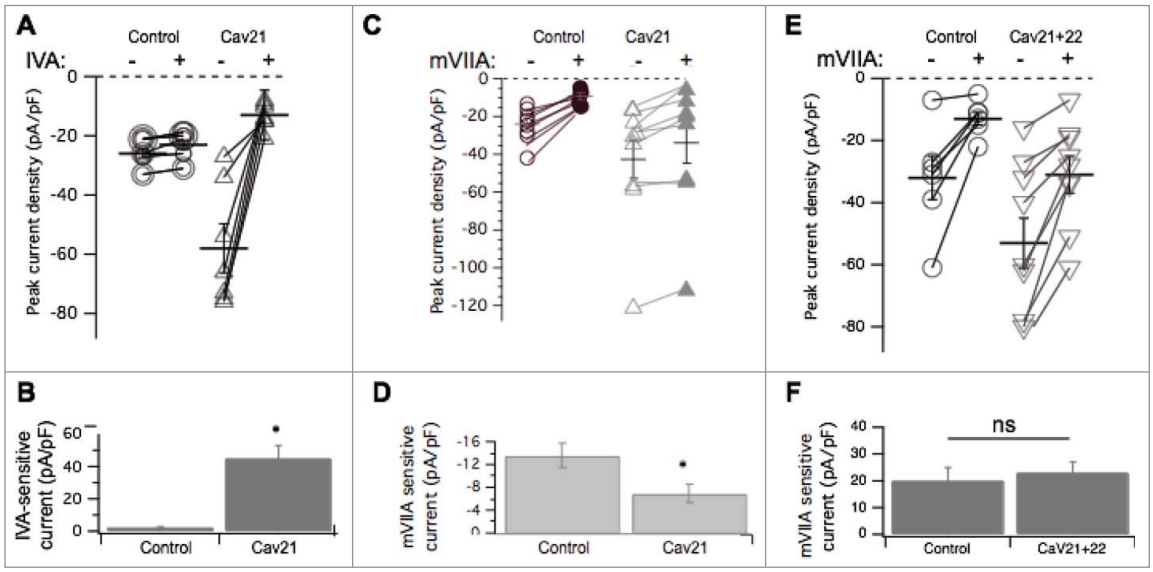

Figure 4. Pharmacological dissection of enhanced calcium currents when $Ca_V2.1$ is expressed in SCG neurons. (A), Summary of control (-) and ω-Agatoxin IVA inhibited (+) current amplitudes in uninjected (○; n = 10), and $Ca_V2.1$- expressing (△; n = 7) SCG neurons. Averages ± standard errors are also indicated as black lines with error bars for each group. (B), Bar graph illustrating average (±SEM) current density inhibited by ω-Agatoxin IVA (total – remaining current) in each group. * indicates p < 0.05. (C), Summary of control (open) and ω-conotoxin mVIIA inhibited (filled) current amplitudes in uninjected (○, •; n = 8), and CaV2.1- expressing (△, ▼; n = 9) SCG neurons. Averages ± standard errors are also indicated as black lines with error bars for each group. (D), Bar graph illustrating average (±SEM) current density inhibited by ω-conotoxin mVIIA (total – remaining current) in each group. (E), Summary of control (open) and ω-conotoxin mVIIA inhibited (filled) current amplitudes in control (○; n = 6), and CaV2.1+CaV2.2- expressing (▽; n = 9) SCG neurons. Averages ± standard errors are also indicated as black lines with error bars for each group. F, Bar graph illustrating average (±SEM) current density inhibited by ω-conotoxin mVIIA (total – remaining current) in each group. * indicates p < 0.05.

under control conditions (Fig. 4A). ω-conotoxin mVIIA, a $Ca_V2.2$ specific blocker, reduced the current by 13 ± 2 pA/pF (n = 19) in uninjected cells, and by 6.9 ± 2 pA/pF (n = 11) in $Ca_V2.1$ expressing cells. This represents a significant reduction in $Ca_V2.2$ current when $Ca_V2.1$ was expressed (p = 0.049 by Student's t test; Fig. 4D). Therefore in contrast to recombinant $Ca_V2.3$, recombinant $Ca_V2.1$ overexpression resulted in reduced $Ca_V2.2$ current compared to uninjected cells. This suggests that recombinant $Ca_V2.1$ displaces some native $Ca_V2.2$ channels, presumably by competing with them for the cellular machinery that regulates their trafficking or membrane stability, or both. In this context, we use the term 'displacement' to suggest only that when $Ca_V2.1$ expression is measurably increased, $Ca_V2.2$ currents decline. The mechanism of this decline is currently unclear and may occur at the level of trafficking of new channels to the membrane, or removal of existing channels more rapidly. Finally, coexpression of recombinant $Ca_V2.2$ with $Ca_V2.1$ prevented displacement of $Ca_V2.2$ current by $Ca_V2.1$. These data are illustrated in Fig. 4E and F along with paired (same day) control cells. Note that while the mVIIA-sensitive current in the control cells was slightly elevated compared to the previous controls, the difference was not significant. On average, the mVIIA-sensitive current in 6 control cells was 20 ± 5 pA/pF and in 9 cells expressing both $Ca_V2.2$ and $Ca_V2.1$, it was 23 ± 4 pA/pF. These values were statistically indistinguishable.

Since $Ca_V2.1$ displaced $Ca_V2.2$ channels but $Ca_V2.3$ did not, and both increased total current, we asked whether these recombinant channels competed with one another for membrane localization. $Ca_V2.1$ and $Ca_V2.3$ cDNA were co-expressed in equal ratios (50 ng/μL of each cDNA) or at 9:1 $Ca_V2.1$: $Ca_V2.3$ (90 ng/μL cDNA and 10 ng/μL cDNA, respectively). Co-expression of $Ca_V2.1$ and $Ca_V2.3$ in both cases increased total current density above control levels significantly (ANOVA; p < 0.01; Fig. 5A), as expected. Average total peak current density was 24 ± 3 pA/pF (n = 17), 52 ± 3 pA/pF (n = 10), and 53 ± 9 pA/pF (n = 6), in uninjected cells and those expressing 1:1 $Ca_V2.1$: $Ca_V2.3$ and 9:1 $Ca_V2.1$: $Ca_V2.3$, respectively

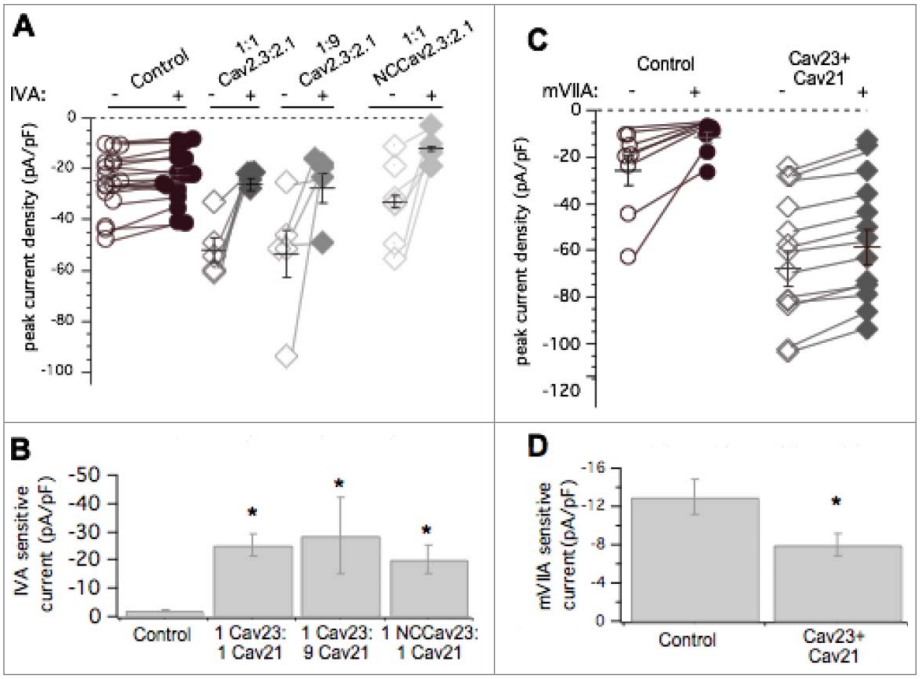

Figure 5. Pharmacological dissection of enhanced calcium currents when both $Ca_V2.3$ and $Ca_V2.1$ are expressed in SCG neurons. (A), Summary of control (open, -) and ω-Agatoxin IVA inhibited (filled, +) current amplitudes in uninjected (○, ●; n = 17) SCG neurons and those expressing $Ca_V2.3$ and $Ca_V2.1$- at 1:1 (◇, ◆ □; n = 5) and 1:9 (◇, ◆ □; n = 5) ratio of cDNA injected, and NCCAV2.3 with $Ca_V2.1$ (◇, ◆ □; n = 6). Averages ± standard errors are also indicated as black lines with error bars for each group. (B), Bar graph illustrating average (±SEM) current density inhibited by ω-Agatoxin IVA (total – remaining current) in each group. * indicates p < 0.05 compared to uninjected controls. (C), Summary of control (open, -) and ω-conotoxin mVIIA inhibited (filled, +) current amplitudes in uninjected (○, ●; n = 8) SCG neurons and those expressing $Ca_V2.3$ and $Ca_V2.1$ together (◇, ◆ □; n = 13). Averages ± standard errors are also indicated as black lines with error bars for each group. (D), Bar graph illustrating average (±SEM) current density inhibited by ω-conotoxin mVIIA (total – remaining current) in each group. * indicates p < 0.05 compared to uninjected controls.

(Fig. 5A). Average ω-agatoxin IVA-sensitive current density (the difference in current before and after the toxin was applied) was 2.2 ± 0.2 pA/pF (n = 17) in uninjected cells, 25 ± 3 pA/pF (n = 10) in cells injected with $Ca_V2.1$: $Ca_V2.3$ at a 1:1 ratio, and 26 ± 12 pA/pF (n = 6), from 9:1 $Ca_V2.1$: $Ca_V2.3$ SCG neurons (Fig. 5B). Co-expression of $Ca_V2.1$ and $Ca_V2.3$ together resulted in significantly larger ω-agatoxin IVA-sensitive current compared to uninjected cells (ANOVA, $p<0.01$). This amount of ω-agatoxin IVA specific current was similar to when $Ca_V2.1$ was expressed alone (Fig. 4A). When NC$Ca_V2.3$ was coexpressed with $Ca_V2.1$ (50 ng/μL of each cDNA), peak current density was 33 ± 2 pA/pF (n = 7), not significantly less than 1:1 $Ca_V2.1$: $Ca_V2.3$ injected cells or cells expressing $Ca_V2.1$ alone (Figs. 4 and 5A; ANOVA, $p<0.01$). Thus we cannot conclude that NC$Ca_V2.3$ channels compete with $Ca_V2.1$ for membrane expression. However, the total current in cells expressing $Ca_V2.1$ alone, $Ca_V2.3$ alone, or both channels together was not significantly different, leaving open the possibility that they may be governed by the same expression ceiling, which is clearly separate from that governing $Ca_V2.2$. Finally, when both $Ca_V2.3$ and $Ca_V2.1$ were overexpressed together, native ω-conotoxin mVIIA-sensitive current was 8.7 ± 1 pA/pF (n = 12), significantly smaller than $Ca_{V2.2}$ current in uninjected cells, which was 13 ± 5 (n = 8; p = 0.031 by Student's t-test; Fig. 5D). This suggests that recombinant $Ca_V2.3$ does not prevent recombinant $Ca_V2.1$ from displacing native $Ca_V2.2$ channels, and thus $Ca_V2.1$ selectively competes with $Ca_V2.2$ for membrane expression. These data suggest that $Ca_V2.2$ is governed by an expression ceiling, and $Ca_V2.3$ by a separate ceiling, while $Ca_V2.1$ expresses more promiscuously, as it appears capable of competing with and displacing both $Ca_V2.2$ and possibly $Ca_V2.3$.

Changes in auxiliary subunits do not underlie differences in recombinant channel expression

Next, we sought to investigate potential mechanisms that governed differential channel expression ceilings. Since recombinant expression of $Ca_V2.2$ did not increase the number of functional channels on the plasma membrane (Fig. 1B), we investigated the limiting mechanism for $Ca_V2.2$. Expressed channels may differentially alter levels of native auxiliary subunits. For example, if native accessory subunit levels are a limiting factor for Ca_V2 expression, it is possible that recombinant $Ca_V2.1$ and $Ca_V2.3$ but not $Ca_V2.2$ may increase these levels, thereby raising the ceiling. RT-PCR analysis indicated all four β subtypes and three $\alpha_2\delta$ subtypes (1-3) were expressed at the message level in SCG neurons (Fig. 6A & B). To determine if auxiliary subunit protein expression was selectively altered, immunocytochemistry (ICC) analysis was

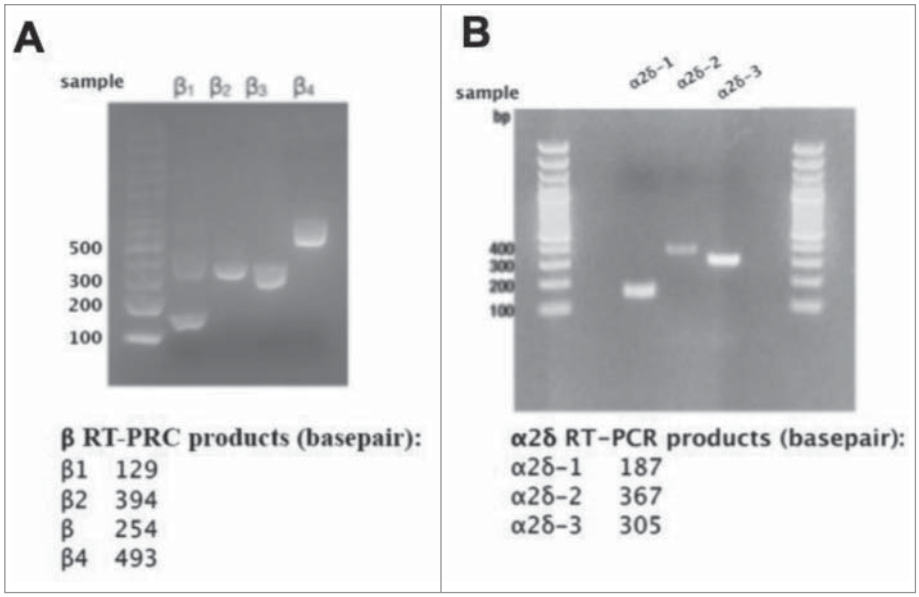

Figure 6. mRNAs for calcium channel β1-4 and $\alpha_2\delta$-1-3 are detectable in RNA isolated from rat SCGs. (A), Agarose gel illustrating results of RT-PCR experiments with specific primers for detection of calcium channel β subunits, as indicated. (B), Agarose gel illustrating results of RT-PCR experiments with specific primers for detection of calcium channel $\alpha_2\delta$ subunits, as indicated. *Lower panels*, Expected product sized for each RT-PCR primer set used in the experiments illustrated above.

conducted to probe expression levels of $\beta 4$ or $\alpha_2\delta$-1 in uninjected, $Ca_V2.2$, or $Ca_V2.3$ expressing cells. To verify that small changes in protein expression would be detectable using ICC, we first performed a time-course experiment in HEK293 cells in which $\beta 4$ was transfected. Cells were fixed and stained for $\beta 4$ at three time points post-transfection (4-, 6-, 8-hours), as protein levels were expected to rise. Representative images of fluorescent HEK cell staining are shown in Fig. 7A. An approximately 5.5-fold increase in fluorescence was detected between the 4- and 8-hour time points using ICC (Fig. 7A, *lower left*). These experiments were corroborated with western blot analysis of HEK293 cells collected in triplicate also at 4-, 6-, and 8 hours post-transfection with $\beta 4$ (Fig. 7A, *right*). The isolated protein was run on a 10% acrylamide gel and the protein density was calculated with normalization to GapDH expression. We were able to detect a 1.5-fold change in protein density between the 4- and 8-hour time points (Fig. 7A). In these experiments, the 4-hour time point is quite close to background fluorescence, as virtually no fluorescence is visible. These data suggest that relatively small changes in protein expression were detectable using ICC.

To determine if overexpression of recombinant Ca_V2 channels differentially altered native expression of auxiliary subunits in SCG neurons, we injected either $Ca_V2.2$ or $Ca_V2.3$ with nuclearly-localized dsRED into isolated SCG neurons. The following day the cells were fixed and stained with antibodies (see *Methods*). Representative images are shown in Fig. 7B. Neurons overexpressing $Ca_V2.2$ had a measurable increase in $\beta 4$ fluorescence compared to uninjected cells (Fig. 7B, *right*), with a ~2-fold increase ($n = 4$) compared to uninjected cells. Similarly, overexpression of $Ca_V2.3$ also resulted in an increase in $\beta 4$, with an observed ~2.53—fold increase in fluorescence compared to uninjected cells ($n = 3$) (Fig. 7B; $p<0.05$ for each respective condition compared to uninjected cell, one-way ANOVA). Interestingly, a decrease in $\alpha 2\delta$-1 fluorescence was observed when $Ca_V2.2$ was overexpressed compared to uninjected cells (Fig. 7C; $p = 0.021$, Student's t-test). With $Ca_V2.3$ overexpression, an apparent decrease was observed in $\alpha_2\delta$-1 fluorescence, but did not reach significance compared to uninjected cells ($n = 4$; $p = 0.062$, by Student's t test) (Fig. 7C). It should be noted that the observed decrease in $\alpha_2\delta$-1 may be due at least in part to masking of the antibody epitope as more Ca_V channels are expressed. Unfortunately, sufficiently high quality antibodies for other channel subunits could not be obtained, so we were limited to analysis of $\alpha_2\delta$-1 and $\beta 4$. Thus when $Ca_V2.2$ or $Ca_V2.3$ was overexpressed, levels of auxiliary subunits $\alpha_2\delta$-1 and $\beta 4$ were altered similarly. It is therefore unlikely that changes in auxiliary subunit availability underlie the observed differences in Ca_V2 channel membrane expression, suggesting the limited ceiling observed for $Ca_V2.2$ overexpression is regulated by another mechanism.

To be certain that these changes, particularly the apparently elevated levels of $\beta 4$ when Ca_V2 channels were expressed, could not explain the differences in recombinant channel expression described above, we heterologously expressed auxiliary subunits alone in SCG neurons and examined whether these would increase calcium current density. In heterologous systems, overexpression of β increases the number of calcium channels trafficked to the plasma membrane,[13] while $\alpha_2\delta$ expression alone does not increase the number of functional channels.[28] It is not clear however, whether similar increases would be evident in neurons that natively express calcium channels with auxiliary subunits. Surprisingly,[29] expression of neither $\beta 4$ alone nor $\alpha_2\delta$-1 alone increased current density in SCG neurons (Fig. 8). However, co-expressing $\beta 4$ with $\alpha_2\delta$-1 did increase current density, although only modestly compared to that seen with $Ca_V2.1$ or 2.3 expression, suggesting more native channels were localized to the plasma membrane (Fig. 8). These data provide a positive control for expression of each auxiliary subunit, but may also indicate that under the conditions of this study, calcium channel auxiliary subunit availability is not the primary limiting factor for Ca_V2 channel ceilings. Therefore, it appears unlikely that the observed increase in native $\beta 4$ levels upon Ca_V2 channel expression is responsible for the selective increase in current upon expression of $Ca_V2.3$ compared with $Ca_V2.2$. However, the decrease in $\alpha_2\delta$ fluorescence in our experiments, as well as research that has supported that $\alpha_2\delta$ is involved with membrane stability and even subcellular trafficking,[30] prompted us to investigate whether auxiliary subunit $\alpha_2\delta$ could affect the selectivity of the calcium channel membrane expression.

Recombinant expression of $\alpha_2\delta$-1 and $\alpha_2\delta$-2 results in preferential trafficking of recombinant Ca_V2 to plasma membrane

To begin to examine the mechanism of selective channel displacement, individual $\alpha_2\delta$ subunits were

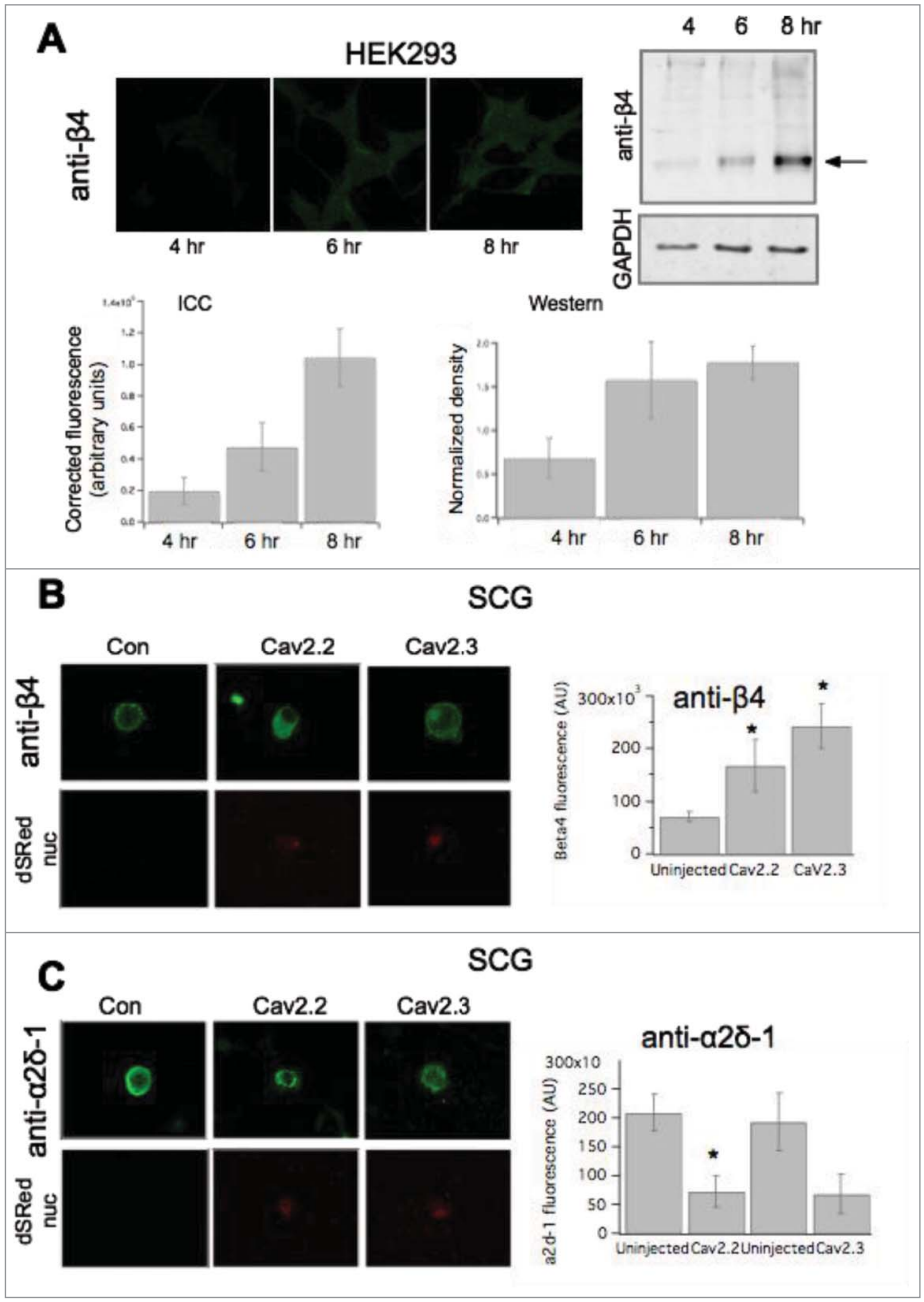

Figure 7. Changes in accessory subunits upon heterologous expression of Ca_V2 channels. (A), Quantification of subunit expression using ICC compared to western blotting. *Upper left*, images showing anti-β4 in HEK293 cells transfected with β4 for 4, 6, and 8 hours, as indicated (see methods for details). *Upper right*, immunoblot showing anti-β4 staining of HEK cell lysates at 4, 6 and 8 hours post transfection. GAPDH loading controls are also shown below. *Lower*, Quantification of HEK cell fluorescence (*left*) and western blot density (*right*) from HEK cells as in *Upper*. (B) *left*, Images showing anti-β4 fluorescence in SCG neurons expressing the indicated Ca_{V2} subunit. *Right*, *upper*, anti-β4 specificity controls showing western blots of HEK cell lysates from cells transfected with the indicated β subunit, or no transfection, as indicated. *Lower*, quantification of ICC data, as in left panel, for control SCG neurons ("uninjected") or expressing $Ca_V2.2$ or $Ca_V2.3$, as indicated. (C), *left*, Images showing anti-$\alpha_2\delta$-1 fluorescence in SCG neurons expressing the indicated Ca_{V2} subunit. Nuclear ds-Red fluorescence is also shown, as an indicator of successfully injected cells. *Right*, quantification of ICC data, as in left panel, for control SCG neurons ("uninjected") or expressing $Ca_V2.2$ or $Ca_V2.3$, as indicated. * indicates $p < 0.05$, vs. control uninjected cells.

expressed alone in SCG neurons, or with specific Ca_V2 channel subtypes, and displacement of $Ca_V2.2$ channels (ω-conotoxin mVIIA sensitive current) was examined. As noted above, expression of $\alpha_2\delta$-1 alone did not detectably alter total current density. Fig. 9A shows a bar graph summary of some of the data described in the figures above, pooled for clarity, including the current sensitive to ω-conotoxin mVIIA

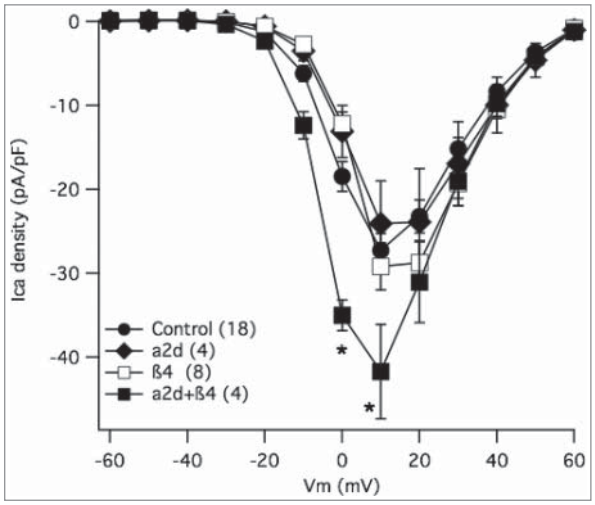

Figure 8. Effect of accessory subunit expression on total calcium current density in SCG neurons. Current-voltage relationship (I-V curves) for control SCG neurons (●), and those expressing $\beta 4$ alone (□), $\alpha_2\delta$-1 alone (◆□), or both subunits together (□). Number of cells in each group is indicated in parentheses in the inset. * indicates $p < 0.05$, vs. control uninjected cells.

(dark gray) and the insensitive current (light gray such that total bar represents the total current) under the indicated Ca_V channel expression conditions. In addition, results from cells expressing $\alpha_2\delta$-1 alone, or with the indicated Ca_V2 channel are shown in Fig. 9B. Expression of $\alpha_2\delta$-1 alone did not change the apparent number of $Ca_V2.2$ channels expressed or total current compared with uninjected cells (Fig. 9B). SCG neurons expressing $\alpha_2\delta$-1 (10 ng/μl) with $Ca_V2.1$ (50 ng/μl) in SCG neurons exhibited increased current density above uninjected cells (** Fig. 9B). $Ca_V2.2$ mediated current remained quite small in neurons expressing both $\alpha_2\delta$-1 and $Ca_V2.1$ (Fig. 9B). The ω-conotoxin mVIIA-sensitive current in these cells was significantly reduced from 15 ± 3 pA/pF ($n = 10$) in cells expressing $\alpha_2\delta$-1 alone to just 5 ± 2 pA/pF ($n = 9$) in $Ca_V2.1/\alpha_2\delta$-1 expressing cells, though the ω-conotoxin mVIIA-sensitive component of the current was not reduced in cells expressing $\alpha_2\delta$-1 alone compared to uninjected cells. Thus, expression of $\alpha_2\delta$-1 with $Ca_V2.1$ seemingly supports the ability of $Ca_V2.1$ to displace native $Ca_V2.2$. Surprisingly, co-expression of $\alpha_2\delta$-1 with $Ca_V2.3$ also reduced $Ca_V2.2$ current. $Ca_V2.2$ currents (mVIIA Ica, dark bars) were 7 ± 1 pA/pF ($n = 11$) in $Ca_{V2.3}/\alpha_2\delta$-1 expressing cells (Fig. 9B). Therefore, $\alpha_2\delta$-1 appears to permit $Ca_V2.2$ displacement by $Ca_V2.3$ ($p = 0.049$ by one-way ANOVA), which does not occur in cells made to

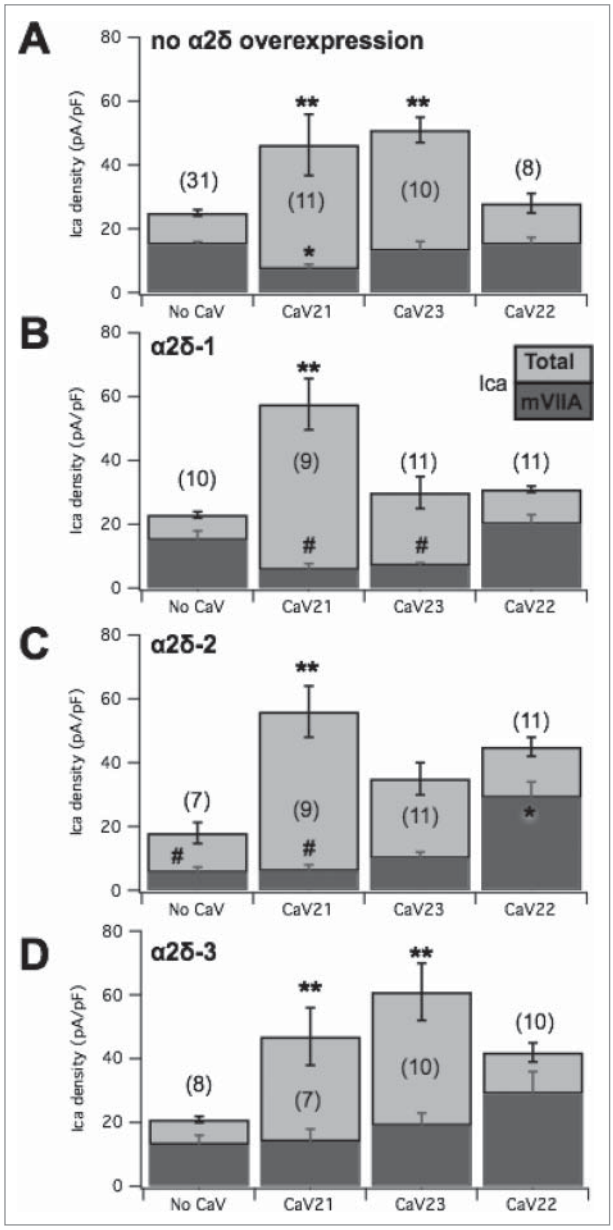

Figure 9. Summary of the effect of $\alpha_2\delta$ subunit expression alone or with Ca_V2 subunits, on total and ω-conotoxin mVIIA sensitive calcium currents in SCG neurons. (A), Pooled data from previous figures illustrating the current densities (total in light gray and ω-conotoxin mVIIA sensitive in dark gray) in uninjected SCG neurons and those expressing each of the Ca_V2 subunits, as indicated. (B), Corresponding data as in (A), but in SCG neurons expressing $\alpha_2\delta$-1 alone ("no Ca_V") and with each of the Ca_V2 subunits, as indicated. (C), Corresponding data as in (A), but in SCG neurons expressing $\alpha_2\delta$-2 alone ("no Ca_V") and with each of the Ca_{V2} subunits, as indicated. (D), Corresponding data as in (A), but in SCG neurons expressing $\alpha_2\delta$-3 alone ("no Ca_V") and with each of the Ca_V2 subunits, as indicated. ** = $p < 0.05$ (ANOVA) for total current density vs. corresponding "No Ca_V" controls; * = $p < 0.05$ (ANOVA) for mVIIA-sensitive current vs. corresponding "No Ca_V" controls; # = $p < 0.05$ (ANOVA) for mVIIA-sensitive current vs. uninjected controls, as shown in panel A. far left.

express $Ca_V2.3$ alone. Finally, expression of $Ca_V2.2$ with $\alpha_2\delta$-1 produced total (30 ± 4 pA/pF) and mVIIA sensitive currents (20 ± 3 pA/pF; n = 11) indistinguishable from control or $\alpha_2\delta$-1 expressing cells. Together, these data indicate that recombinant $\alpha_2\delta$-1 expression enhances $Ca_V2.2$ displacement by other Ca_V2 channels, but does not alter the $Ca_V2.2$ ceiling.

We then asked whether recombinant expression of other $\alpha_2\delta$ proteins could alter channel displacement properties in SCG neurons. $\alpha_2\delta$-2 was expressed in SCG neurons alone and with $Ca_V2.1$ or $Ca_V2.3$. Similar to results with $\alpha_2\delta$-1, $\alpha_2\delta$-2 expressed alone was not associated with a significant change in total current density (18 ± 3 pA/pF; n = 7; Fig. 9C). There was however a significant reduction in the amount of current sensitive to ω-conotoxin mVIIA compared to uninjected cells, dropping to 5 ± 2 pA/pF (n = 7). In addition, co-expression of $Ca_V2.1$ with $\alpha_2\delta$-2 resulted in enhanced total current, and the ω-conotoxin mVIIA-sensitive current was just 6 ± 2 pA/pF (n = 9), similar to the reduced current in cells expressing $\alpha_2\delta$-2 alone (Fig. 9C). Expression of $Ca_V2.3$ and $\alpha_2\delta$-2 together resulted in 10 ± 2 pA/pF (n = 11) ω-conotoxin mVIIA-sensitive current, not significantly smaller than $\alpha_2\delta$-2 alone (Fig. 9C), but note that this value was reduced from control cells. Interestingly, both the total current (45 ± 7 pA/pF) and the mVIIA-sensitive current (29 ± 5 pA/pF; n = 11) were significantly elevated in cells expressing $Ca_V2.2$ with $\alpha_2\delta$-2 (Fig. 9C), suggesting that it may raise the ceiling for $Ca_V2.2$ expression, although the fact that the current was not elevated when $\alpha_2\delta$-2 was expressed alone indicates that the role of $\alpha_2\delta$-2 in governing the ceiling is complex. Thus, these data suggest that $\alpha_2\delta$-2, like $\alpha_2\delta$-1, allows recombinant $Ca_V2.1$ displacement of native $Ca_V2.2$ channels but permits elevated $Ca_V2.2$ channel expression.

When expressed alone, $\alpha_2\delta$-3 did not alter total membrane current (Fig. 9D) or the current sensitive to ω-conotoxin mVIIA compared with uninjected cells. The total current density in these cells was 21 ± 4 pA/pF, and the ω-conotoxin mVIIA sensitive current was 13 ± 3 pA/pF (n = 8; Fig. 9D). When $\alpha_2\delta$-3 was co-expressed with $Ca_V2.1$, the total and ω-conotoxin mVIIA sensitive current was 47 ± 8 and 14 ± 4 pA/pF, respectively (n = 7) (Fig. 9D). With $\alpha_2\delta$-2 and $Ca_V2.3$ co-expressed, the total current was 60 ± 8 pA/pF, and ω-conotoxin mVIIA reduced the current by 19 ± 4 pA/pF (n = 10) (Fig. 9D). Thus, the ω-conotoxin mVIIA sensitive current when $\alpha_2\delta$-3 is co-expressed alone or with either $Ca_V2.1$ or $Ca_V2.3$ is not significantly altered. Next, $\alpha_2\delta$-3 expressing SCG neurons were also injected with recombinant $Ca_V2.2$ (Fig. 9D). Perhaps surprisingly, neither the ω-conotoxin mVIIA sensitive current (27 ± 7 pA/pF) nor the total current (40 ± 10 pA/pF; n = 10) was significantly altered compared with uninjected cells or cells expressing $\alpha_2\delta$-3 alone. This was perhaps due to the variability, because clearly the average values were quite high. We confirmed the function of $\alpha_2\delta$-3 by expressing this construct with $Ca_V2.2$ and β4 in HEK293 cells (not shown), which confirmed a significant increase in current density was observed compared to $Ca_V2.2/\beta$4 co-expression, consistent with reports that $\alpha_2\delta$-3 stabilizes Ca_V channel expression on the plasma membrane.[28] Thus, our data suggest that $\alpha_2\delta$-3, in contrast with $\alpha_2\delta$-1, appears to "protect" native $Ca_V2.2$ channels from displacement by recombinant channels for plasma membrane expression, but perhaps does not raise the specific $Ca_V2.2$ expression ceiling. Overall, our data suggest that each $\alpha_2\delta$ uniquely alters the relationship between Ca_V2 channel expression priority in SCG neurons. These data highlight a novel, subtype-specific role for $\alpha_2\delta$ proteins in differentially prioritizing membrane expression of various Ca_V2 channels, although a great deal more work will be needed to fully understand the distinct trafficking mechanisms that regulate Ca_V channels and the specific roles of the $\alpha_2\delta$ subunits in these processes.

Discussion

The goal of this study was to determine if there were discernible patterns of somatic Ca_V2 channel membrane expression in rat SCG neurons. Many expression and trafficking studies regarding Ca_V2 channels have been limited to presynaptic expression[17,19,20]. With many presynaptic-specific interactions it could be possible that those studies overlooked instances of selectivity between Ca_V2 subtypes that occur outside of the presynapse.

We found that in the time frame of these studies, $Ca_V2.2$ is limited with respect to the number of channels that functionally express at the plasma membrane, unlike $Ca_V2.1$ and $Ca_V2.3$ whose expression can be elevated by the introduction of recombinant channel protein. The selective ability of recombinant $Ca_V2.1$ and $Ca_V2.3$ (but not $Ca_V2.2$) to enhance

current density in SCG neurons did not appear to result from changes in expression of native Ca_V auxiliary subunits, at least in a simple way, as both $Ca_V2.2$ and $Ca_V2.3$ overexpression appeared to alter the expression of $\alpha_2\delta$-1 and β4 similarly (Fig. 7), and overexpression of individual $\alpha_2\delta$ or β subunits alone did not increase current density (Figs. 8 & 9). Unfortunately, due to the limitations of available antibodies, we could not test for changes in every subunit, so we cannot definitively rule that out as a mechanism for the selective effects we measured, but based on the data we do have, this seems unlikely. Since auxiliary subunits do not appear to be limiting when recombinant $Ca_V2.2$ is overexpressed, there is likely another mechanism limiting channels expressed on the plasma membrane. This subtype is the dominant channel in adult SCG neurons, and primarily induces neurotransmission.[17] Therefore it is plausible that there are additional requirements for this channel to be trafficked to the plasma membrane, or the channel is segregated to be trafficked to the presynapse exclusively. In dorsal root ganglia (DRG) sensory neurons it was established that splice isoforms have differential membrane expression patterns.[23] This is not likely related to the mechanism of enhanced current density observed with $Ca_V2.1$, as the 37a variant of that channel does not result in larger current densities than the 37b variant (data not shown). Therefore, particular protein interactions with those isoforms are clearly essential to determining the number of channels trafficked to the plasma membrane. A limitation in these proteins could perhaps induce the ceilings observed in this study. There have been some indications of proteins that interact with Ca_V2 channels in a subtype dependent manner, though investigation on their influence on selective membrane expression over other Ca_V2 subtypes needs to be pursued in further detail[31,32].

Further, we found that $Ca_V2.1$, but not $Ca_V2.3$, reduces the amount of native $Ca_V2.2$ expressed on the plasma membrane. This selective ability of recombinant $Ca_V2.1$ to displace native $Ca_V2.2$ was studied in more detail. Interestingly, we found that displacement appeared to depend on $\alpha_2\delta$ subunits in a subtype specific way (Fig. 9). While expression of $\alpha_2\delta$-1, $\alpha_2\delta$-2 or $\alpha_2\delta$-3 alone did not alter current density, expression of $\alpha_2\delta$-1 and $\alpha_2\delta$-2 seemed to allow $Ca_V2.1$ to displace native $Ca_V2.2$ and $\alpha_2\delta$-1 permitted displacement by recombinant $Ca_V2.3$ when it was co-expressed. By contrast, expression of $\alpha_2\delta$-3 produced the opposite effect, protecting native $Ca_V2.2$ channels from displacement by other Ca_V2 channels. These findings demonstrate a novel effect of $\alpha_2\delta$ subtypes in conferring preference on Ca_V2 channel subtype functional expression. At this time, it is unclear exactly what the 'displacement' process entails, so we can only interpret what we actually measure: that when $Ca_V2.1$ is expressed, for example, there is less mVIIA sensitive current. One possibility is that the rate of turnover of $Ca_V2.2$ protein is unchanged, but recombinant $Ca_V2.1$ competes with native $Ca_V2.2$ during trafficking for insertion into the plasma membrane. Alternatively, expression of recombinant $Ca_V2.1$ may get to the membrane by a separate mechanism or pathway, then cause loss of native $Ca_V2.2$ by some other mechanism, possibly by accelerating removal (reducing the half-life of the existing protein). It will be interesting to better understand the details of these processes in the future.

Trafficking studies on Ca_V2 channels have focused heavily on presynaptic localization.[6] The presynapse is incredibly small and highly organized,[33] and localization of calcium channels near the neurotransmitter machinery is essential for efficient neurotransmission. Further, certain subtypes are preferentially expressed at the presynapse over others[17,19]. One hypothesis that describes this subtype selectivity is the "slot" hypothesis. In mouse hippocampal neurons, recombinant $Ca_V2.2$ overexpression did not increase neurotransmission, measured as excitatory post-synaptic potential (EPSC) amplitude, but overexpression of $Ca_V2.2$ reduced $Ca_V2.1$-mediated neurotransmission. Further, overexpression of $Ca_V2.1$ was not able to displace $Ca_V2.2$-mediated channels at the synapse. Thus, it was hypothesized that there are $Ca_V2.2$ -specific "slots" and $Ca_V2.1$-preferring "slots", with "slots" being undetermined cellular limitations that regulate the amount of Ca_V2 subtype that mediates neurotransmission at the presynapse. It is very interesting that we observe parallels in the present study. At the somatic membrane, we observe a limitation in the amount of $Ca_V2.2$ mediated current, and possibly a selectivity, or preference, for recombinant $Ca_V2.1$ over native $Ca_V2.2$ channels. While our experiments were conducted in adult rat SCG neurons that do not express native $Ca_V2.1$, at least in the cell body, the interplay between subtype selectivity for membrane expression is reminiscent of the results in Cao and Tsien's study. Pointedly, the selectivity preferences are opposite for

each respective study, suggesting that there may be cell-specific preferences for Ca_V2 subtype expression, or that selective expression (displacement) depends on different factors at the cell body and the synapse. Interestingly, Hoppa et al.[20] confirmed that $Ca_V2.1$ overexpression in hippocampal neurons did not cause displace $Ca_V2.2$ channels at the synapse, but did lead to increased current density at the cell body, a finding that mirrors what we report in sympathetic neurons here, lending support to the idea that similar mechanisms are in play in both neuronal subtypes, but with strikingly different outcomes in the two cellular compartments.

At the cell body of SCG neurons, it is tempting to speculate that there are at least two separate 'compartments' (not necessarily a physical space but perhaps a combination of trafficking circumstances and physical localization on the plasma membrane) for channel expression because 1) N-channels are the predominant natively expressed channel, but heterologous expression of $Ca_V2.2$ does not increase current density, and 2) heterologous expression of $Ca_V2.3$, the other natively expressed channel, can increase current density but does not displace native N-channels. We could tentatively call these the "N" compartment and the "R" compartment. It will be interesting in the future to evaluate what the nature of these compartments may be, and how they are shaped by $\alpha_2\delta$ subunits. We may speculate that the N compartment may consist of channels on the soma that are destined for trafficking to synaptic sites, while those in the R compartment will reside only on the somatic membrane. This assumption would be accompanied by certain predictions that could be tested. For example, native $Ca_V2.2$, but not 2.3 channels would likely be associated with presynaptic proteins such as RIM-1. While the complexity of the results presented here indicate that $\alpha_2\delta$ subunits are unlikely to be the sole regulators of channel expression in each compartment, the differential effects on channel expression suggest that they play some regulatory role. Perhaps most interestingly was that expression of each $\alpha_2\delta$ subunit resulted in a different profile of channel expression with respect to channel expression and ability to displace native $Ca_V2.2$ channels. Table 1 shows a preliminary assessment of Ca_V2 channel type expression in each putative compartment based on the data obtained to date. Note that because these assessments are based primarily on 1) displacement of native N-currents and 2) enhancement of total current, they are not thorough enough to rule out alternate models that could explain the data. For example, the increase in mVIIA sensitive current when $\alpha_2\delta$-2 and $Ca_V2.2$ are coexpressed (Fig. 9C) could be explained by a higher ceiling for the N compartment, or by allowing $Ca_V2.2$ channels to express in the R compartment. In Table 1, we interpret it as the latter since expression of $\alpha_2\delta$-2 alone does not appear to raise the N compartment ceiling. Regardless, the data do provide evidence that SCG neurons appear to produce, traffic, and/or sort channels in a manner that is influenced by $\alpha_2\delta$ subunits in a subtype specific way.

Table 1. Categorization of differential effects on Ca_V2 channel expression by $\alpha_2\delta$ subunits.

		No $\alpha_2\delta$	$\alpha_2\delta$-1	$\alpha_2\delta$-2	$\alpha_2\delta$-3
"N" compartment	$Ca_V2.1$	√	√	√	
	$Ca_V2.2$	√	√	√	√
	$Ca_V2.3$		√		
"R" compartment	$Ca_V2.1$	√	√	√	√
	$Ca_V2.2$			√	
	$Ca_V2.3$	√			√

A mechanism that explains the subtype selectivity in the "slot" hypothesis at presynapses has yet to be described in detail. The auxiliary subunit $\alpha_2\delta$ created a "bottleneck" or limitation in Ca_V2 localization to the presynapse,[20] so it is interesting that we found a Ca_V2 selectivity preference based on various $\alpha_2\delta$s. Though it is not explicitly demonstrated, it is possible that $\alpha_2\delta$s are not only the limiting factor in presynaptic membrane localization, but also the mechanism by which selectivity is conferred for presynaptic Ca_V2 subtype expression.

Many circumstances could arise to employ the $\alpha_2\delta$-1 selectivity mechanism for Ca_V2 expression. For example, $\alpha_2\delta$-1 can serve as the receptor for thrombospodin,[34] a protein involved in developing synapses, or LRP-1 to influence Ca_V channel trafficking.[35] It was also theorized that $\alpha_2\delta$-1 serves as an initial organizer for the synapse.[34] It may be possible then the $Ca_V2.1$ is selectively chosen for presynaptic expression in newly developed or developing synapses. For example, in SCG neurons cultured from P0 rats, $Ca_V2.1$ is present at the presynapse along with $Ca_V2.2$. Thus, $\alpha_2\delta$-1 may permit the expression of $Ca_V2.1$ at the presynapse. However, to date preferential association of $\alpha_2\delta$ subunits with Ca_V channels has not been demonstrated. Thus, we propose that the selectivity may arise

in a more limited, but still important circumstance. One of the known roles of $\alpha_2\delta$ subunits in regulating Ca_V channels is to promote recycling from the endosomal compartment.[30] Because $\alpha_2\delta$ associates with the extracellular regions of the channel, it would reside within the unique low pH environment inside the endosome. It is possible that in this environment, selectivity of $\alpha_2\delta$-Ca_V channel association is more pronounced and could underlie the phenomena we observe here in which specific $\alpha_2\delta$ subunits appear to selectively prioritize Ca_V channel membrane expression. Since only a small fraction of channel complexes are expected to reside in the endosome at any given time, this kind of limited selectivity may have eluded detection using standard biochemical methods. A more thorough test of this hypothesis will be a priority in future studies.

Materials and methods

SCG isolation

The neuronal isolation and injection procedures are from established protocols. SCG were dissected from adult male Wistar rats (175-200 g) and incubated in Earle's balanced salt solution (Life Technologies, Rochelle, MD) containing 0.55 mg/ml trypsin (Worthington, Freehold, NJ), and 1.5 mg/ml Type IV collagenase (Worthington) for 1 hour at 35°C. Cells were collected through centrifugation and transferred to minimum essential medium (Fisher Scientific, Pittsburgh, PA). The cells were then plated, and incubated at 37°C until cDNA injection. All animal protocols were approved by the University of Rochester's Committee on Animal Resources (UCAR).

cDNA injection

Injection of cDNA occurred roughly 4–6 hours after cell isolation. cDNA injections were performed with an Eppendorf 5247 microinjector and Injectman NI2 micromanipulator (Madison, WI). Plasmids were stored at −20°C as a 1–2 μg/μl stock solution in TE buffer (10 mM TRIS, 1 mM EDTA, pH 8). Cells were then incubated at 37°C following injection and experiments are performed the following day.

The rabbit α1B (Ca_V2.2) clone was obtained from Stephen Ikeda (NIAAA, NIH). The exon 37 splice variants for rat α1B were obtained from Addgene (Cambridge, MA) (plasmid #: 26567, 37a; 26569, 37b). The α1A (Ca_V2.1) clone was obtained from Stephen Ikeda (NIAAA, NIH). The human α1E (Ca_V2.3) clone was obtained from Stephen Ikeda (NIAAA, NIH). The rat $\alpha_2\delta$-1 clone was obtained from Stephen Ikeda (NIAAA, NIH). The mouse $\alpha_2\delta$-2 (plasmid #58732) and mouse $\alpha_2\delta$-3 (plasmid #58728) clones were purchased from Addgene (Cambridge, MA). The β4 plasmid was obtained from Stephen Ikeda (NIAAA, NIH). All α1 plasmids were injected at 100 ng/μL unless otherwise indicated. Auxiliary subunits $\alpha 2\delta$ and β cDNA was injected at 10 ng/μL unless otherwise indicated. All neurons were co-injected with green fluorescent protein cDNA (50 ng/μl; pEGFPC1; Clontech Laboratories, Palo Alto, CA, USA) to identify cells expressing recombinant protein.

Electrophysiology data acquisition and analysis

Patch-clamp recordings were made using 8250 glass (King Precision Glass, Claremont, CA). Pipette resistances were 0.8-3 MΩ yielding uncompensated series resistances of 1–5 MΩ. Series resistance compensation of $\geq$ 80% was used in all recordings. Data was recorded using an Axopatch 200B patch-clamp amplifier (Molecular Devices, Sunnyvale, CA). Voltage protocol generation and data acquisition were performed using custom procedures written for the Igor Pro software package (Wavemetrics, Lake Oswego, OR) generously provided by Stephen R. Ikeda (NIH, NIAAA) on a Mac OSX Intel Duocore computer with an Instrutech ITC-18 data acquisition board (HEKA Instruments, now Harvard Bioscience, Holliston, MA). Currents were sampled at 100 kHz, low-pass filtered at 5 kHz, and digitized. Data was stored and analyzed offline. All currents were leak subtracted off line prior to data analysis. All patch-clamp experiments were performed at room temperature (21–24°C). The external (bath) calcium current recording solution contained (in mM):145 tetraethylammonium (TEA) 140methanesulfonate, 10 4-(2-Hydroxyethyl)-1-piperazineethanesulfonic acid (HEPES), 15 glucose, 10 $CaCl_2$, and 300 nMtetrodotoxin, pH 7.4, osmolality 320 mOsm/kg. The internal (pipette) solution contained: 120 N-methyl-Dglucamine (NMG), 20 TEA, 11 EGTA, 10 HEPES, 10 sucrose, 1 $CaCl_2$, 4 Mg-ATP, 0.3 Na_2-GTP, and 14 tris-creatine phosphate, pH 7.2, osmolality 300 mOsm/kg.

Data analysis was performed using Igor Pro software (WaveMetrics, Lake Oswego, OR). Using whole-

cell patch-clamp electrophysiology, the total amount of functional channels on the plasma membrane in each expression condition was determined by application of 80 msec voltage steps ranging from −80 mV to +60 mV in 10 mV increments from a holding potential (V_{hold}) of −80 mV. The calcium currents were measured 10 msec after the start of each step, at or near steady-state levels, normalized to cell capacitance and plotted against voltage, generating a current-voltage (IV) curve. Currents did not appreciably inactivate during this time. To determine the amount of each Ca_{V2} subtype contributing to the total calcium current, one or more selective pharmacological inhibitors were perfused on the cell while a voltage ramp (−120 mV to 80 mV in 160 msec from a holding potential of −80 mV) was applied every ten seconds until maximum inhibition was achieved. The relative amount of current blocked by that inhibitor represented subtype population functionally expressing on the plasma membrane. Non-specific binding was blocked by applying cytochrome-c from equine heart (90+%) (1 mg/mL; Alfa Aesar, Haverhill, MA). Additionally, all drugs were diluted into external calcium solution with cytochrome-c (1 mg/mL). Concentrations of pharmacological agents perfused were as indicated in the text. Cells were excluded if the leak current at −80 mV was >10% of the peak inward calcium current during a voltage ramp.

Molecular biology and RT-PCR

$Ca_V2.2$ and $Ca_V2.3$ were rendered non-conductive through site directed mutagenesis using PfuUltra II Hotstart PCR MasterMix (Agilent Technologies, Santa Clara, CA) followed by DpnI digestion. The mutations done for $Ca_V2.2$ in the mouse α1B37B exon clone were at amino acids E344A, E693A, E1392A and E1682A. Mutations in human $Ca_V2.3$ α1E clone were at amino acids E309A, E657A, E1374A and E1665A.

Total RNA from adult rat SCG neurons purified using RNAeasy (Qiagen, Hilden, Germany). RT-PCR was done usingOneStep RT-PCR (Qiagen) following manufacturers protocols. PCR products were run on 2% agarose gel (ThermoFisher Scientific, Waltham, MA) diluted into 1X TAE Electrophoresis Buffer (ThermoFisher Scientific, Waltham, MA). Primers used for β were: β1 forward (5′) AGGGCTCA GCAGAGTCC, β1 reverse (5′) AGAAAG CCAAGACCAAACC, β2 forward (5′) GCATGTTA AGGAAAAATTTAATAATG, β2 reverse (5′) AAGAAGACAGAGCACACTCC, β3 forward (5′) AGGCGGGTTCAGCCGACTC, β3 reverse (5′) ATTTTCTGCACATTAAAGAGAAG, β4 forward (5′) AGCGAAGTCCAAACCTG, β4 reverse (5′) ATGAGGTAACAGACATGATGC. Primers used for $\alpha_2\delta$ were: $\alpha_2\delta$-2 forward (5′) CAAGGACAATCG-GAACCTGTTT, $\alpha_2\delta$-2 reverse (5′) TGACGGTA-GAGCCTTTGTAGA, $\alpha_2\delta$-1 forward (5′) CAAGTCA TGGGTGGATAAAATG, $\alpha_2\delta$-1 reverse (5′) TGC AATTTCAACCAGTTGGCG, $\alpha_2\delta$-3 forward (5′) CA CTTCAGGGAGCATTTGGA, $\alpha_2\delta$-3 reverse (5′) GTG GAGATCTGGGTGAAAAA.

HEK cell culture

Human embryonic kidney 293 (HEK 293) cells were maintained in Dulbecco's Modified Eagle Medium (DMEM) supplemented with 5% Fetal Bovine Serum (FBS) (Atlas Biologics, Fort Collins, CO) and 2% Penicillin/Streptomycin (MP Biomedicals, LLC, Solon, OH) in a humidified incubator with 5% CO_2. Cells were passed using 0.25% Trypsin (Thermo Fischer Scientific, Waltham, MA) following standard procedures. HEK293 cells were transfected using polyethylenimine (PEI).

Western blotting

Western blots were performed using polyacrylamide gels containing 30% acrylamide (Biorad Hercules, CA), 10% Ammonium persiflage (APS; Biorad), Temed (Biorad), Separating buffer (1.5M Tris base, pH 8.8, 0.4% SDS) (Boston Bioproducts, Ashland, MA), Stacking buffer (0.5M Tris-HCl, pH 6.8, 0.4% SDS) (Boston Bioproducts). 8 or 10% acrylamide gels were run at ∼100 V for twenty minutes, then 40–80 minutes at 120V until protein was adequately through the gel. Protein product was transferred to nitrocellulose membrane (Biorad) in −20°C at 100 V for one hour. The membrane was blocked with 30% milk (Sturm Foods, Manawa, WI) diluted in TBS (19 mMTris base, pH 7.5, 137 mMNaCl, 2.7 mMKCl, 5% Tween-20 (Biorad), before the primary antibody was applied. Primary antibodies were diluted into TBS with 10% milk. Primary antibody was applied overnight at 4°C while rocking. Following four 5 minute washes with TBS, secondary antibody, also diluted in TBS with 10% milk, was applied. After a hour incubation at room temperature, the secondary antibody was

washed four times with TBST. Membranes were scanned on a Li-Cor Odyssey (Lincoln, NE) and data was stored and analyzed offline using Igor Pro software (WaveMetrics, Lake Oswego, OR). For densitometry analysis, lines were analyzed based on density. Values for background were subtracted for each lane. Protein bands were normalized to GapDH signal strength. Antibody specificity was confirmed using HEK293 cells expressing each β subunit separately or mock transfected (not shown), and for $\alpha_2\delta$-1 by examining lysates from neural tissue, which express $\alpha_2\delta$ subunits, and adipose tissue, which does not (not shown).

Immunocytochemistry

For analyzing auxiliary subunit expression, neurons were isolated, cultured on cover slips were injected with Ca_V2 $\alpha1$ subtype of interest with nuclearly-localized ds-Red (acquired from Dr. David I. Yule, University of Rochester) for identification. Procedure for immunocytochemistry for isolated cells was guided by published protocols.[36] Following overnight culture, cells were fixed with 5 minute application of −20°C chilled acetone (Mallinckrodt Chemicals, St. Louis, MI) followed by 0.01M glycine (Sigma Aldrich, St. Louis, MO) in 1X phosphate buffered saline (PBS; Corning Life Sciences, Tewksbury, MA) for 5 minutes. After a brief wash with 1X PBS cells were permeabilized with triton-X100 (Sigma Aldrich, St. Louis, MO) for 5 minutes and subsequently washed twice with 1X PBS for 1 minute. 1X PBS with 10% bovine serum albumin (BSA; Sigma Aldrich) was used to block non-specific binding for 30 minutes before overnight application (16-18 hours) of primary antibody. The following day cells underwent four 5 minute washes with 1X PBS, followed by 1 hour incubation with the secondary antibody. After four 5 minute washes with PBS, the coverslips were placed on slides with ProLongGold AntifadeMountant (Molecular Probes) and stored at −80° C until use.

Chemical depolarization was induced with potassium chloride solution, as optimized and described for SCG neurons previously.[37] SCG neurons were plated onto coverslips and cultured overnight. To induce depolarization, cells were washed with elevated potassium chloride (KCl) solution ranging from 40–90 mM for 15 seconds, then washed with 5 mMKCl solution for 45 seconds. Cells were then fixed and stained as described. The solution, based on Tyrode's solution, was as follows (in mM): 115 NaCl, 40 KCl, 2 $MgCl_2$, 2 $CaCl_2$, 10 Hepes, 10 glucose, pH 7.3), with variation in NaCl and KCl concentrations ensuring adequate osmolarity. Pre-treatment with1 μM SNX-482 (Alomone Labs, Jerusalem, Israel) 500 nM ω-conotoxin mVIIA (Tocris Bioscience, Avonmouth, Bristol, UK) or cytochrome-c from equine heart (90+%) (1 μg/μL; Alfa Aesar, Haverhill, MA) diluted in external calcium solution was performed five minutes prior to depolarization.

Antibodies

Anti-$\alpha_2\delta$-1 rabbit polyclonal antibody (1:200) was obtained from Alomone (catalog #ACC-015). Anti-GapDH rabbit polyclonal antibody (1:2500) was obtained from Abcam (catalog #ab9485, Cambridge, MA). Anti-phospho-CREB (SER133) (87G3) rabbit monoclonal antibody (1:133) was obtained from Cell Signaling Technologies (catalong #9198; Danvers, MA). Anti-β4 mouse monoclonal antibody (1:250) was obtained from Abcam (catalog #ab85788). Alexa Fluor 488 goat anti-rabbit IgG (1:10,000) was obtained from Life Technologies (catalog #A11008; Rochelle, MD). Alex Fluor 488 goat anti-mouse (1:10,000) was obtained from Life Technologies (catalog #A11001). Dylight 800 Anti-rabbit IgG (1:10,000) was obtained from Thermo-Fischer (catalog #SA5-35571; Rockford, IL).

Imaging

Immunofluorescence images were obtained using a TILL Photonics digital imaging system that was ported to a NikonEclipseTi epifluorescent microscope. Fluorescence was measured using a 40x oil immersion objective lens. Confocal images were obtained using EZ-C1 3.60 software (Nikon, Melville, NY). Cells were excited with argon lasers at wavelengths 488 nm and 543 nm. Signal was detected via dichroic mirror on the image plane with 530 ± 30 or 585 ± 30 band pass filter for Alexafluor488 or dsRed, respectively. Images were analyzed with FIJI (Image J). Corrected total cell fluorescence (CTCF) was calculated by measuring the area of the cell, the integrated density of that area and mean fluorescence of the background. The formula used was CTCF = Integrated Density – (Area of selected cell X mean fluorescence of background reading), as described in the literature.[38]

Statistics

Statistical significance was determined with unpaired Student's t-test (2-tail) for two sample experiments or

one-way ANOVA (unweighted) to compare means across multiple samples. P values ≤ 0.05 were considered significant. Group means and standard deviations from experiments were used in Power calculations http://www.biomath.info/power/ttest.htm to utilize statistical tests ($a = 0.05$ and power $= 0.8$) estimating the minimum number of cells necessary for each experiment. Curve fitting was done using Igor Pro software (Wavemetrics, Lake Oswego, OR). Linear fits used the equation $y = a+bx$. Gaussian distributions were fit to $y = Aexp[-((x- xo)/width)2]$.

Disclosure of potential conflicts of interest

No potential conflicts of interest were disclosed.

Acknowledgments

We thank Lyndee Knowlton for technical assistance, D. I. Yule (University of Rochester) for use of and assistance with the confocal microscope, R. T. Dirksen, M. E. Dumont, and A. Grossfield (University of Rochester) for helpful discussions.

Funding

Funded by NIH R01 GM101023, to PJK.

References

[1] Catterall WA. Voltage-gated calcium channels. Cold Spring Harb Perspect Biol. 2011;3:a003947. doi:10.1101/cshperspect.a003947. PMID:21746798

[2] Zhu Y, Ikeda SR. Adenosine modulates voltage-gated Ca2+ channels in adult rat sympathetic neurons. J Neurophysiol. 1993;70:610-20. PMID:8410161

[3] Beqollari D, Kammermeier PJ. The interaction between mGluR1 and the calcium channel Cav(2).(1) preserves coupling in the presence of long Homer proteins. Neuropharmacology. 2013;66:302-10. doi:10.1016/j.neuropharm.2012.05.038. PMID:22659088

[4] Dolphin AC. Voltage-gated calcium channels and their auxiliary subunits: physiology and pathophysiology and pharmacology. J Physiol 2016;594:5369-90. doi:10.1113/JP272262. PMID:27273705

[5] Rettig J, Sheng ZH, Kim DK, Hodson CD, Snutch TP, Catterall WA. Isoform-specific interaction of the alpha1A subunits of brain Ca2+ channels with the presynaptic proteins syntaxin and SNAP-25. Proc Natl Acad Sci U S A. 1996;93:7363-8. doi:10.1073/pnas.93.14.7363. PMID:8692999

[6] Wu LG, Westenbroek RE, Borst JG, Catterall WA, Sakmann B. Calcium channel types with distinct presynaptic localization couple differentially to transmitter release in single calyx-type synapses. J Neurosci. 1999;19:726-36. PMID:9880593

[7] Ma H, Groth RD, Wheeler DG, Barrett CF, Tsien RW. Excitation-transcription coupling in sympathetic neurons and the molecular mechanism of its initiation. Neurosci Res. 2011;70:2-8. doi:10.1016/j.neures.2011.02.004. PMID:21352861

[8] Wheeler DG, Groth RD, Ma H, Barrett CF, Owen SF, Safa P, Tsien RW. Ca(V)1 and Ca(V)2 channels engage distinct modes of Ca(2+) signaling to control CREB-dependent gene expression. Cell. 2012;149:1112-24. doi:10.1016/j.cell.2012.03.041. PMID:22632974

[9] Dolphin AC. Calcium channel auxiliary alpha2delta and beta subunits: trafficking and one step beyond. Nat Rev Neurosci. 2012;13:542-55. doi:10.1038/nrn3317. PMID:22805911

[10] Arikkath J, Campbell KP. Auxiliary subunits: essential components of the voltage-gated calcium channel complex. Curr Opin Neurobiol. 2003;13:298-307. doi:10.1016/S0959-4388(03)00066-7. PMID:12850214

[11] Cole RL, Lechner SM, Williams ME, Prodanovich P, Bleicher L, Varney MA, Gu G. Differential distribution of voltage-gated calcium channel alpha-2 delta (alpha2delta) subunit mRNA-containing cells in the rat central nervous system and the dorsal root ganglia. J Comp Neurol. 2005;491:246-69. doi:10.1002/cne.20693. PMID:16134135

[12] Bichet D, Cornet V, Geib S, Carlier E, Volsen S, Hoshi T, Mori Y, De Waard M. The I-II loop of the Ca2+ channel alpha1 subunit contains an endoplasmic reticulum retention signal antagonized by the beta subunit. Neuron. 2000;25:177-90. doi:10.1016/S0896-6273(00)80881-8. PMID:10707982

[13] Waithe D, Ferron L, Page KM, Chaggar K, Dolphin AC. Beta-subunits promote the expression of Ca(V)2.2 channels by reducing their proteasomal degradation. J Biol Chem. 2011;286:9598-611. doi:10.1074/jbc.M110.195909. PMID:21233207

[14] Davies A, Douglas L, Hendrich J, Wratten J, Tran Van Minh A, Foucault I, Koch D, Pratt WS, Saibil HR, Dolphin AC. The calcium channel alpha2delta-2 subunit partitions with CaV2.1 into lipid rafts in cerebellum: implications for localization and function. J Neurosci. 2006;26:8748-57. doi:10.1523/JNEUROSCI.2764-06.2006. PMID:16928863

[15] Kasai H. Cytosolic Ca2+ gradients, Ca2+ binding proteins and synaptic plasticity. Neurosci Res. 1993;16:1-7. doi:10.1016/0168-0102(93)90002-8. PMID:8251011

[16] Schweizer FE, Betz H, Augustine GJ. From vesicle docking to endocytosis: intermediate reactions of exocytosis. Neuron. 1995;14:689-96. doi:10.1016/0896-6273(95)90213-9. PMID:7718232

[17] Mochida S, Westenbroek RE, Yokoyama CT, Zhong H, Myers SJ, Scheuer T, Itoh K, Catterall WA. Requirement for the synaptic protein interaction site for reconstitution of synaptic transmission by P/Q-type calcium channels. Proc Natl Acad Sci U S A. 2003;100:2819-24. doi:10.1073/pnas.262787699. PMID:12601156

[18] Cao YQ, Piedras-Renteria ES, Smith GB, Chen G, Harata NC, Tsien RW. Presynaptic Ca2+ channels compete for channel type-preferring slots in altered

neurotransmission arising from Ca2+ channelopathy. Neuron. 2004;43:387-400. doi:10.1016/j.neuron.2004.07.014. PMID:15294146

[19] Cao YQ, Tsien RW. Different relationship of N- and P/Q-type Ca2+ channels to channel-interacting slots in controlling neurotransmission at cultured hippocampal synapses. J Neurosci. 2010;30:4536-46. doi:10.1523/JNEUROSCI.5161-09.2010. PMID:20357104

[20] Hoppa MB, Lana B, Margas W, Dolphin AC, Ryan TA. alpha2delta expression sets presynaptic calcium channel abundance and release probability. Nature. 2012;486:122-5. PMID:22678293

[21] Lu VB, Williams DJ, Won YJ, Ikeda SR. Intranuclear microinjection of DNA into dissociated adult mammalian neurons. J Vis Exp. 2009. doi:10.3791/1614. PMID:20010540

[22] Hodgkin AL, Huxley AF, Katz B. Measurement of current-voltage relations in the membrane of the giant axon of Loligo. J Physiol. 1952;116:424-48. doi:10.1113/jphysiol.1952.sp004716. PMID:14946712

[23] Castiglioni AJ, Raingo J, Lipscombe D. Alternative splicing in the C-terminus of CaV2.2 controls expression and gating of N-type calcium channels. J Physiol. 2006;576:119-34. doi:10.1113/jphysiol.2006.115030. PMID:16857708

[24] Macabuag N, Dolphin AC. Alternative Splicing in Ca(V)2.2 Regulates Neuronal Trafficking via Adaptor Protein Complex-1 Adaptor Protein Motifs. J Neurosci. 2015;35:14636-52. doi:10.1523/JNEUROSCI.3034-15.2015. PMID:26511252

[25] Newcomb R, Palma A, Fox J, Gaur S, Lau K, Chung D, Cong R, Bell JR, Horne B, Nadasdi L, et al. SNX-325, a novel calcium antagonist from the spider Segestria florentina. Biochemistry. 1995;34:8341-7. doi:10.1021/bi00026a015. PMID:7541240

[26] Olivera BM, Cruz LJ, de Santos V, LeCheminant GW, Griffin D, Zeikus R, McIntosh JM, Galyean R, Varga J, Gray WR, et al. Neuronal calcium channel antagonists. Discrimination between calcium channel subtypes using omega-conotoxin from Conus magus venom. Biochemistry. 1987;26:2086-90.

[27] Mintz IM, Venema VJ, Swiderek KM, Lee TD, Bean BP, Adams ME. P-type calcium channels blocked by the spider toxin omega-Aga-IVA. Nature. 1992;355:827-9. doi:10.1038/355827a0. PMID:1311418

[28] Cassidy JS, Ferron L, Kadurin I, Pratt WS, Dolphin AC. Functional exofacially tagged N-type calcium channels elucidate the interaction with auxiliary alpha2delta-1 subunits. Proc Natl Acad Sci U S A. 2014;111:8979-84. doi:10.1073/pnas.1403731111. PMID:24889613

[29] Kadurin I, Alvarez-Laviada A, Ng SF, Walker-Gray R, D'Arco M, Fadel MG, Pratt WS, Dolphin AC. Calcium currents are enhanced by alpha2delta-1 lacking its membrane anchor. J Biol Chem. 2012;287:33554-66. doi:10.1074/jbc.M112.378554. PMID:22869375

[30] Tran-Van-Minh A, Dolphin AC. The alpha2delta ligand gabapentin inhibits the Rab11-dependent recycling of the calcium channel subunit alpha2delta-2. J Neurosci. 2010;30:12856-67. doi:10.1523/JNEUROSCI.2700-10.2010. PMID:20861389

[31] Ferron L, Nieto-Rostro M, Cassidy JS, Dolphin AC. Fragile X mental retardation protein controls synaptic vesicle exocytosis by modulating N-type calcium channel density. Nat Commun. 2014;5:3628. doi:10.1038/ncomms4628. PMID:24709664

[32] Grauel MK, Maglione M, Reddy-Alla S, Willmes CG, Brockmann MM, Trimbuch T, Rosenmund T, Pangalos M, Vardar G, Stumpf A, et al. RIM-binding protein 2 regulates release probability by fine-tuning calcium channel localization at murine hippocampal synapses. Proc Natl Acad Sci U S A. 2016;113:11615-20. doi:10.1073/pnas.1605256113. PMID:27671655

[33] Augustine GJ, Santamaria F, Tanaka K. Local calcium signaling in neurons. Neuron. 2003;40:331-46. doi:10.1016/S0896-6273(03)00639-1. PMID:14556712

[34] Eroglu C, Allen NJ, Susman MW, O'Rourke NA, Park CY, Ozkan E, Chakraborty C, Mulinyawe SB, Annis DS, Huberman AD, et al. Gabapentin receptor alpha2delta-1 is a neuronal thrombospondin receptor responsible for excitatory CNS synaptogenesis. Cell. 2009;139:380-92. doi:10.1016/j.cell.2009.09.025. PMID:19818485

[35] Kadurin I, Rothwell SW, Lana B, Nieto-Rostro M, Dolphin AC. LRP1 influences trafficking of N-type calcium channels via interaction with the auxiliary alpha2delta-1 subunit. Sci Rep. 2017;7:43802. doi:10.1038/srep43802. PMID:28256585

[36] Glynn MW, McAllister AK. Immunocytochemistry and quantification of protein colocalization in cultured neurons. Nat Protoc. 2006;1:1287-96. doi:10.1038/nprot.2006.220. PMID:17406413

[37] Wheeler DG, Barrett CF, Groth RD, Safa P, Tsien RW. CaMKII locally encodes L-type channel activity to signal to nuclear CREB in excitation-transcription coupling. J Cell Biol. 2008;183:849-63. doi:10.1083/jcb.200805048. PMID:19047462

[38] McCloy RA, Rogers S, Caldon CE, Lorca T, Castro A, Burgess A. Partial inhibition of Cdk1 in G 2 phase overrides the SAC and decouples mitotic events. Cell Cycle. 2014;13:1400-12. doi:10.4161/cc.28401. PMID:24626186